

promoting access to White Rose research papers



Universities of Leeds, Sheffield and York
<http://eprints.whiterose.ac.uk/>

This is the author's post-print version of an article to be published in the **Journal of Alloys and Compounds**

White Rose Research Online URL for this paper:

<http://eprints.whiterose.ac.uk/id/eprint/78224>

Published article:

Castle, EG, Mullis, AM and Cochrane, RF (2013) *Evidence for an extended transition in growth orientation and novel dendritic seaweed structures in undercooled Cu-8.9 wt%Ni*. Journal of Alloys and Compounds. ISSN 0925-8388 (In Press)

<http://dx.doi.org/10.1016/j.jallcom.2013.12.088>

Evidence for an extended transition in growth orientation and novel dendritic seaweed structures in undercooled Cu-8.9wt%Ni

Elinor G. Castle^a, Andrew M. Mullis^b, Robert F. Cochrane^c

^aInstitute of Materials Research, University of Leeds, Leeds LS2 9JT, UK.

pm07egc@leeds.ac.uk

^bInstitute of Materials Research, University of Leeds, Leeds LS2 9JT, UK.

A.M.Mullis@leeds.ac.uk

^cInstitute of Materials Research, University of Leeds, Leeds LS2 9JT, UK.

R.F.Cochrane@leeds.ac.uk

Corresponding author:

Elinor Castle. IMR, School of Process and Environmental and Materials Engineering, Engineering building, University of Leeds, Leeds, LS2 9JT, UK. pm07egc@leeds.ac.uk.
+44(0)113 343 2391 or +44(0)7891519694.

Abstract

A melt encasement (fluxing) technique has been used to systematically study the microstructural development and velocity-undercooling relationship of a Cu-8.9wt%Ni alloy at undercoolings up to 235 K. A complex series of microstructural transitions have been identified with increasing undercooling. At the lowest undercoolings a <100> type dendritic structure gives way to an equiaxed grain structure, consistent with the low undercooling region of grain refinement observed in many alloys. At intermediate undercoolings, dendritic growth returns, consisting of dendrites of mixed <100> and <111> character. Within this region, 8-fold growth is first observed at low undercoolings, indicating the dominance of

<100> character. As undercooling is increased, <111> character begins to dominate and a switch to 6-fold growth is observed. It is believed that this is an extended transition region between <100> and <111> dendrite growth, the competing anisotropies of which are giving rise to a novel form of dendritic seaweed, characterised by its containment within a diverging split primary dendrite branch. At higher undercoolings it is suggested that a transition to fully <111> oriented dendritic growth occurs, accompanied by a rapid increase in growth velocity with further increases in undercooling. At the highest undercooling achieved, a microstructure of both small equiaxed grains, and large elongated grains with dendritic seaweed substructure, is observed. It is thought that this may be an intermediate structure in the spontaneous grain refinement process, in which case the growth of dendritic seaweed appears to play some part.

Keywords

Metals and alloys, rapid-solidification, anisotropy, microstructure, metallography

1. Introduction

In the study of rapid solidification from undercooled metallic melts, spontaneous grain refinement has been observed to occur in many different metal and alloy systems, including Ni, Ni-Cu, Cu-O, Ge and Fe-Co [1-5]. Here, an abrupt transition from a coarse columnar to a fine grained equiaxed structure is observed above a critical undercooling ΔT^* . In many alloys, e.g. Ni-Cu [2] and Cu-O [3], a further transition, from equiaxed grains at low undercooling to columnar grains at intermediate undercoolings, is observed.

A number of theories for the fundamental origins of spontaneous grain refinement have been proposed [3, 6-8], the most widely accepted currently being the surface energy driven remelting and fragmentation process proposed by Schwarz et al. [9] which is based on the

stability analysis of Karma [10]. However, the theoretical basis for the Karma model has since been brought into question by Mullis et al. [11] who later proposed that spontaneous grain refinement could be due to the development of growth instabilities above ΔT^* , resulting in a transition in growth mode from dendritic to dendritic seaweed [12]. This is an inherently unstable structure which is likely to remelt post-solidification, forming many solid islands on which new grains could nucleate. It is known to arise in situations where competing anisotropies in the growth direction become comparable in strength [13]. Such situations have been observed with increasing undercooling in Cu-Sn [14] and Ge-Fe [15] alloys, in which it appears that the competition between two differently directed anisotropies facilitates an abrupt change in growth direction as their strength becomes comparable. It is possible, therefore, that such conditions may also favour the growth of dendritic seaweed under certain circumstances.

In order to help illuminate the possible origins of spontaneous grain refinement, the present report investigates the growth velocity (V) vs. undercooling (ΔT) relationship of a Cu-8.9wt%Ni alloy using a containerless, melt-fluxing technique. Detailed microstructural and texture analysis of the as-solidified samples was carried out in order to identify any transitions in preferred growth orientation or dendrite morphology with increasing undercooling.

2. Material and methods

A Cu-Ni alloy was prepared from compacted high purity 99.999% metals basis Cu and Ni powders by arc-melting under inert argon atmosphere. X-ray fluorescence (XRF) and light element combustion analysis (LECO[®]) confirmed a final composition of Cu-8.9wt%Ni with a residual oxygen concentration of 0.237 wt%.

Full details of the melt-fluxing equipment and procedure are given elsewhere [14], however, the basic procedure involves the cyclic heating of spherical samples 5-6 mm in diameter, under inert nitrogen atmosphere. Samples were suspended in a molten flux of 60wt% B₂O₃ – 40wt% Na₂SiO₃, previously mixed and dewatered at 1073 K, and contained within a small fused-silica crucible. The flux ensured that no contact was made between sample and crucible, limiting the number of potential heterogeneous nucleation sites and increasing the level of undercooling attainable. Temperature was monitored by means of an r-type thermocouple as samples were subjected to thermal cycling. This consisted of superheating to around 130 K above the liquidus temperature to ensure full melting of the alloy and removal of bubbles from the glass flux. The sample was held at this temperature for 15 min, before slow-cooling at an average rate of 10 K/min until solidification was spontaneously nucleated. High-speed digital imaging (up to 15 000 fps) was then used to calculate the velocity of the recalescence front in order to investigate the velocity-undercooling relationship of this alloy. Microstructural analysis using optical microscopy (Olympus BX51 microscope, fitted with a Carl Zeiss AxioCam MRc5 camera) and SEM imaging using a Carl Zeiss EVO MA15 SEM was performed on the as-solidified samples in order to investigate the nucleation points and any other significant features evident on the surface of the droplets. Droplet interior microstructures were then imaged in bright field, dark field and DIC optical microscopy modes, following precision sectioning and polishing. In cases where the nucleation point was visible on the surface of the droplet, sectioning could be performed with a well-defined orientation relative to the growth direction. Select samples were then subjected to XRD texture analysis via pole figure plots, generated by a Phillips/PanAlytical diffractometer (Cu K α radiation) equipped with a texture stage.

3. Results and discussion

Detailed microstructural analysis has revealed the existence of a complex series of growth transitions with increasing undercooling. Starting with the lowest undercoolings observed (up to around $\Delta T = 45$ K) droplets consisted of single grains comprising of dendritic substructures, an example of which is shown in figure 1 (top), a sample undercooled by $\Delta T = 35$ K. The orthogonal morphology of dendrites observed within this range of undercooling suggests a $\langle 100 \rangle$ growth orientation, in line with the more usual form of dendritic growth expected for the FCC Cu-Ni system.

Between $45 \text{ K} \leq \Delta T \leq 85 \text{ K}$, an equiaxed grain structure is observed, in which coarse parent grains appear to consist of smaller sub-grains. A DIC micrograph of a sample undercooled by $\Delta T = 65$ K is shown in figure 1 (bottom) in which broad, light and dark regions indicate the parent grains, and some sub-grain boundaries can be observed. A dendritic substructure is evident in this image and appears to cross the grain boundaries. This is confirmed by the inset $\{200\}$ pole figure which exhibits only one set of poles, indicating that the dendritic substructure is continuous throughout. Furthermore, the existence of curved grain boundaries is indicative of grain boundary migration. Hence it is suggested that some post-solidification grain coarsening has occurred, consistent with the recrystallisation mechanism associated with the low undercooling region of grain refinement observed in many alloys.

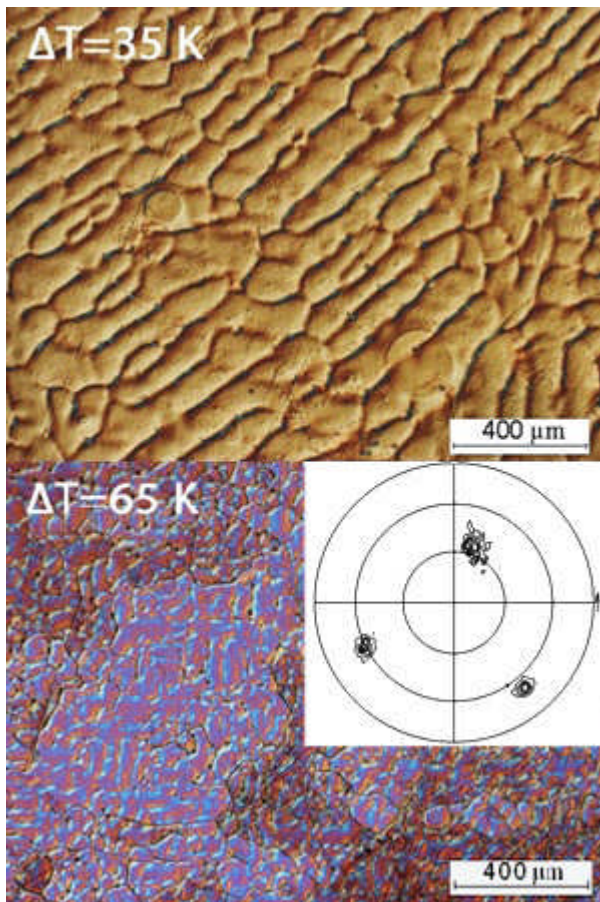


Figure 1. Optical bright-field micrograph of a Cu-8.9wt%Ni sample undercooled by $\Delta T = 35$ K (top) and DIC micrograph of a sample undercooled by $\Delta T = 65$ K (bottom), with inset $\{200\}$ pole figure.

Above $\Delta T = 85$ K, a transition back to dendritic growth was observed and clear nucleation points were apparent on the sample surfaces. Up to around $\Delta T = 155$ K, the nucleation points mostly exhibited 8-fold symmetry, as shown in figure 2 (top left), an optical microscope image of a sample undercooled by $\Delta T = 139$ K. Here, a mixture of $\langle 100 \rangle$ and $\langle 111 \rangle$ type growth appears to be present. Feature 1 shows a split primary dendrite branch with orthogonal outer secondary branches, suggesting $\langle 100 \rangle$ type growth, whilst feature 2 indicates a primary branch at 90° to this, exhibiting non-orthogonal secondaries, indicating a possible $\langle 111 \rangle$ orientation. $\{200\}$, $\{220\}$ and $\{111\}$ pole figures were taken from this sample. None of these plots exhibited a central pole, most likely as a result of slightly off-axis

sectioning, and hence the growth orientation could not be concluded. However, what is evident from the pole figures is the presence of a second grain which appears to be twinned about one of the $\{111\}$ directions, as shown by the two sets of poles mapped out on the $\log\{111\}$ pole figure (figure 2, top right).

As undercooling is increased above $\Delta T = 155$ K, a transition to a 6-fold nucleation pattern is observed, as shown in figure 2 (bottom left) an optical microscope image of a sample undercooled by $\Delta T = 161$ K. Again, neighbouring primary branches of opposing orientation are observed, however in this sample a primary branch is, unusually, seen to exhibit orthogonal secondary branches on one side and non-orthogonal on the opposite (feature 1). The $\log\{111\}$ pole figure (bottom right) has a strong pole at its centre, indicating a dominant $\langle 111 \rangle$ growth orientation. An investigation into the 7 poles observed on the pole figure reveals a possible triple-twin relationship between three grains. Poles 1-4 represent one grain, since they share common angles of either 72° or 109° with each other. Through the same relationship poles 4, 5 and 6 and poles 6, 2 and 7 constitute the remaining two grains. Hence each grain shares a common pole with each of the other two (either pole 2, 4 or 6).

In all samples between $85 \text{ K} \leq \Delta T \leq 205 \text{ K}$ a novel form of dendritic seaweed is observed. This structure is seen as features 3.i and 3.ii in figure 2 (top left) and in feature 2 (bottom left), an SEM montage of which is shown in figure 3. This structure appears to originate from a diverging split primary branch, the inner secondaries of which appear to have bent to become near-parallel with the primary direction of the branch, subsequently undergoing repeated tip splitting. The result is a dendritic seaweed structure which appears bound by dendrite branches. In some cases, such as with features 3.i (top left) and 2 (bottom left) in figure 2, there are orthogonal outer secondary branches on the split primary branch. In these cases the seaweed terminates in an array of parallel dendrites, as can be seen in figure 3. In

other cases, such as with feature 3.ii, no outer secondary branches are seen, and in this instance the seaweed structure appears to break down via the growth of $\langle 111 \rangle$ type dendrites.

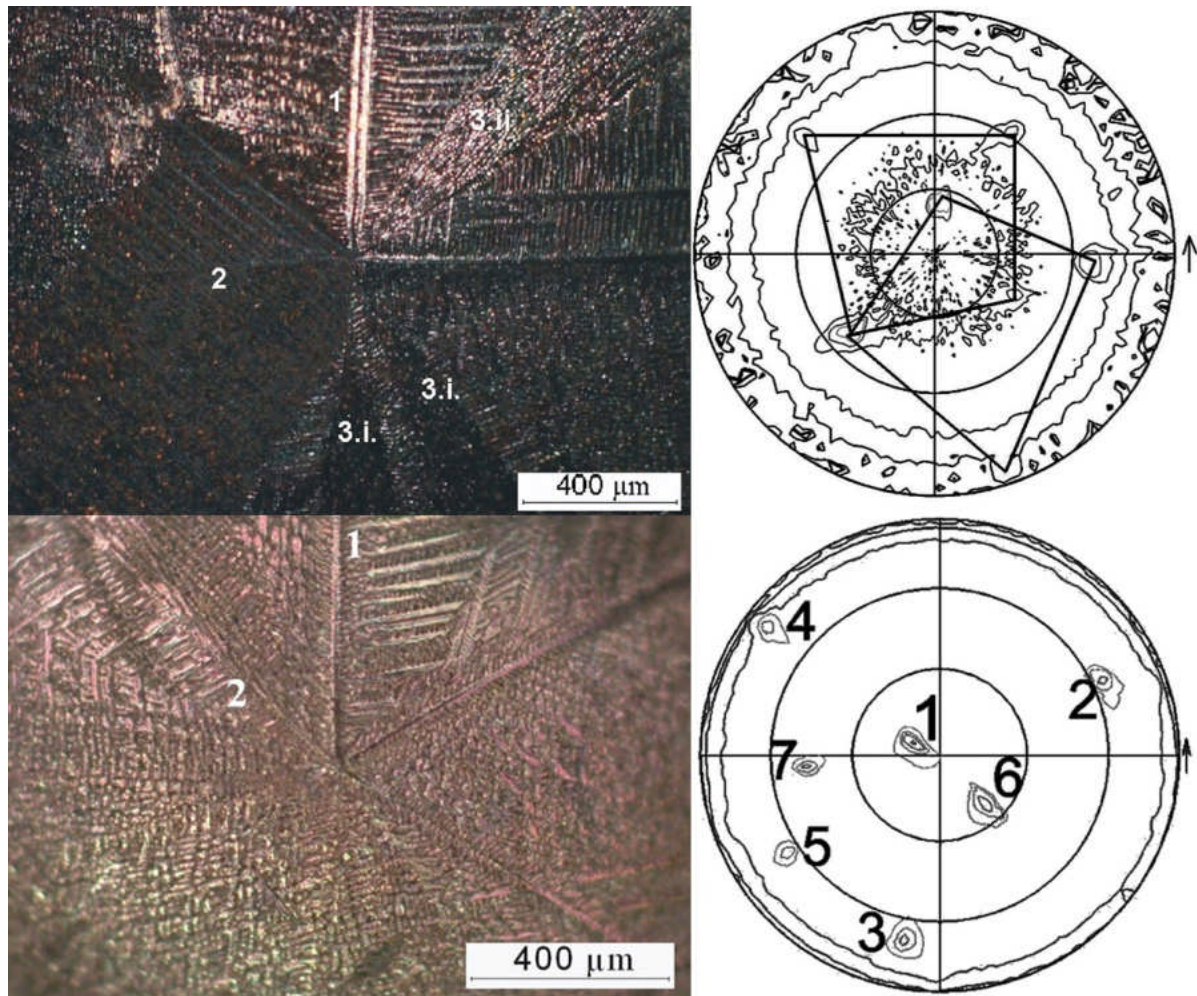


Figure 2. Optical micrographs of (top left) 8-fold nucleation pattern on the surface of a sample of Cu-8.9wt%Ni sample undercooled by $\Delta T = 139$ K and (bottom left) 6-fold nucleation pattern observed on the surface of a sample undercooled by $\Delta T = 161$ K. To the right are the corresponding $\log\{111\}$ pole figures.

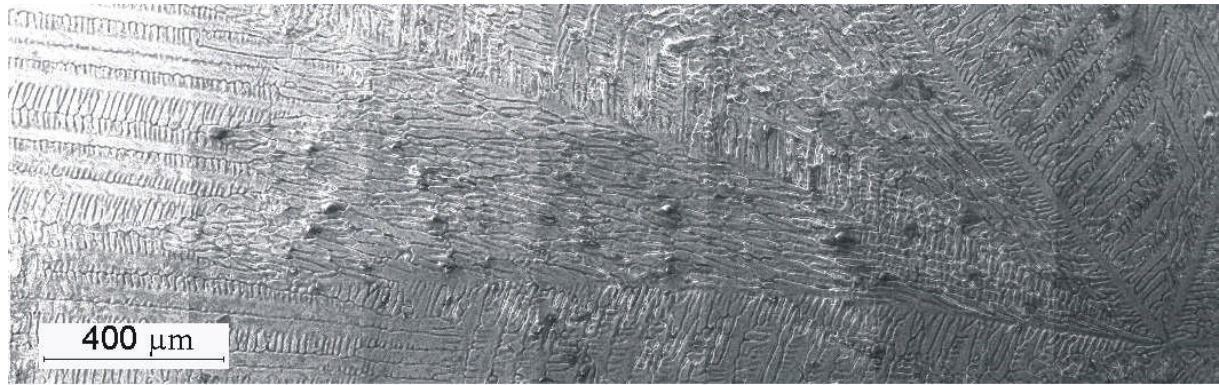


Figure 3. An SEM montage of the branch of seaweed observed in the sample undercooled by 161 K, labelled as feature ‘2’ in figure 3 (bottom left).

At around $\Delta T = 205$ K, a transition to a coarse-grained structure is seen (figure 4, top left), consisting of a dendritic substructure which appears to be discontinuous between grains. This is confirmed by the inset $\{111\}$ pole figure which exhibits several sets of poles, indicating the presence of several grains, between which no orientational relationship can be found.

As undercooling is increased, at around 220 K a transition to a finer grain structure is observed, as seen in figure 4 (right) showing an optical dark field image of a sample undercooled by 220 K. Some directionality appears present in this sample, with grains transitioning from equiaxed to elongated morphologies from right to left (approx.). This is reflected in the inset $\{111\}$ pole figure showing a large number of poles which are mostly confined to one half of the plot. The bright region in the centre of the droplet is due to the porosity of the sample in this area. Under DIC it becomes apparent that the majority of the droplet has an underlying dendritic substructure, which is very seaweed-like in regions of elongated grains, as shown in figure 4 (bottom left). In addition, many of the equiaxed grains appear devoid of any discernable substructure.

Since a global transformation to fine equiaxed grains has not occurred, this sample is not considered to be grain refined. However it may represent an intermediate structure in the grain refinement process, in which case, dendritic seaweed appears to play an important part.

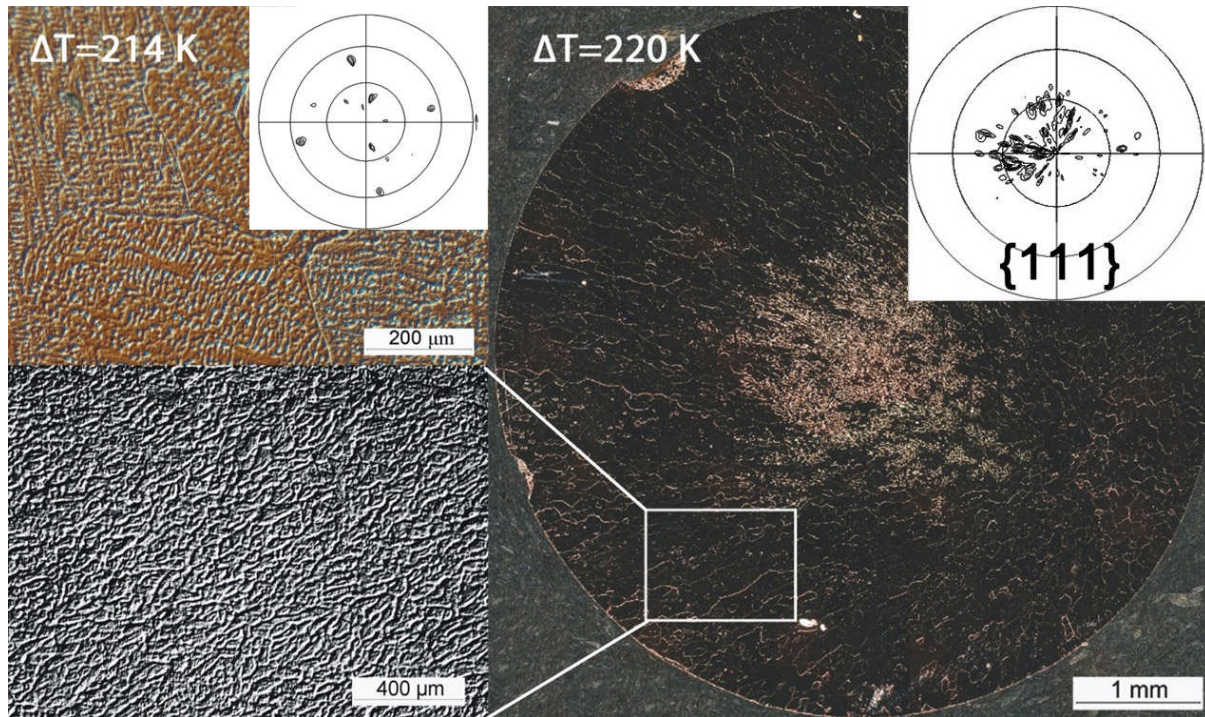


Figure 4. (Top left) DIC micrograph of a Cu-8.9wt%Ni sample undercooled by $\Delta T = 214 \text{ K}$ with inset $\{111\}$ pole figure, (right) optical dark field micrograph of a sample undercooled by $\Delta T = 220 \text{ K}$ with inset $\{111\}$ pole figure and (bottom left) enhanced DIC micrograph of dendritic seaweed observed in the region marked on the $\Delta T = 220 \text{ K}$ image.

A summary of the growth morphologies and transition undercoolings, together with the associated growth velocity as a function of undercooling is given in Fig. 5. From the data it is difficult to unambiguously identify any clear breaks in the velocity-undercooling curve that might be associated with a change in growth direction. This is perhaps somewhat surprising in a system that is variously showing 4-, 6- and 8- fold symmetry and preferred orientation along both the $\langle 100 \rangle$ and $\langle 111 \rangle$ directions. However, there is a rapid acceleration of the

growth velocity for undercoolings in excess of 210 K (from 40 m s^{-1} to 94 m s^{-1} over a 30 K interval), which might be associated with a switch to the faster $\langle 111 \rangle$ growth direction.

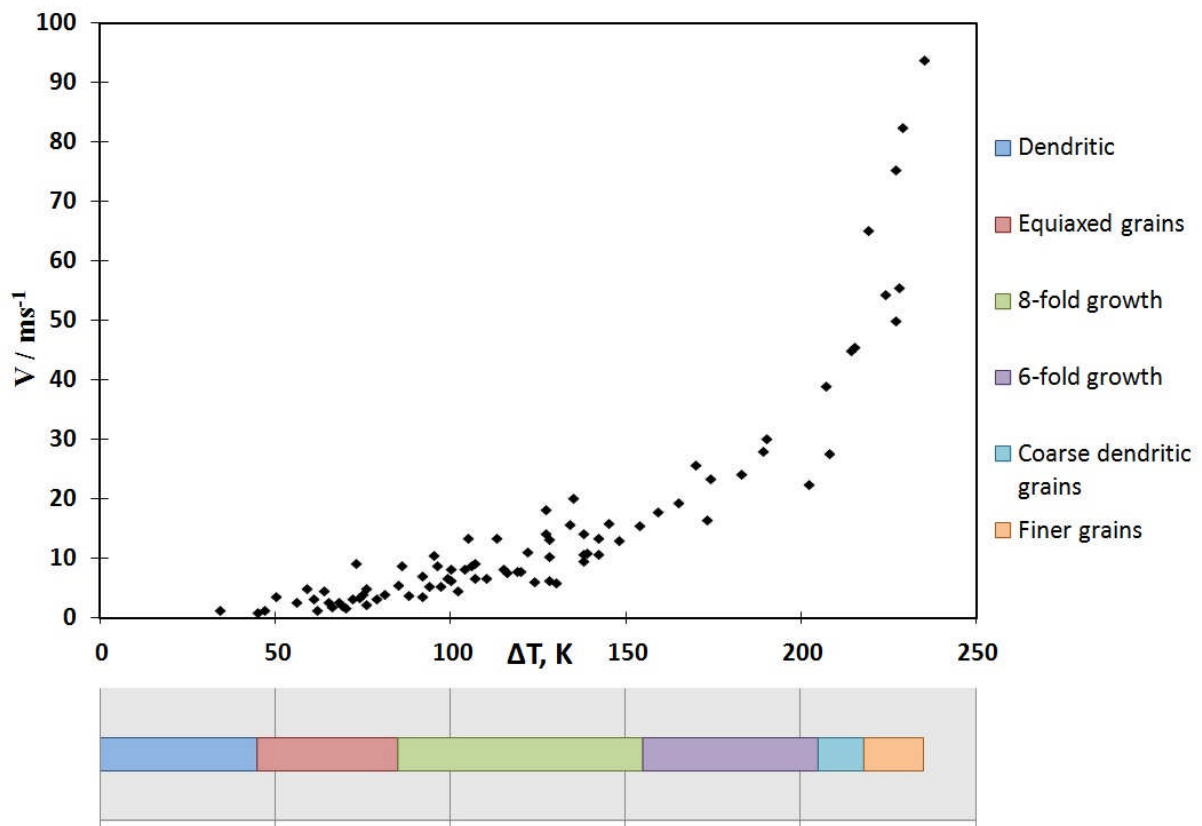


Figure 5. Velocity-undercooling relationship and microstructural transitions observed in Cu-8.9wt%Ni.

4. Further discussion

The results presented above suggest that, at intermediate undercoolings there appears to be some competition between anisotropies in the $\langle 100 \rangle$ and $\langle 111 \rangle$ growth directions. This is resulting in the twin-assisted growth of mixed-orientation microstructures and appears to be giving rise to the observed ‘branches’ of dendritic seaweed.

It is suggested that we are observing a considerably extended transition between $\langle 100 \rangle$ growth at low undercooling and $\langle 111 \rangle$ growth at high undercooling. In the intermediate

region, 8-fold growth suggests that $\langle 100 \rangle$ character is dominating at low undercooling, with a transition to 6-fold growth at high undercooling indicating the increasing dominance of $\langle 111 \rangle$ character. If so, it may be that the transition between the 6-fold growth regime and coarse-grained regime at $\Delta T = 205$ K corresponds to a transition to fully $\langle 111 \rangle$ growth. This would be consistent with the rapid increase in growth velocity observed above $\Delta T = 210$ K. However, post-solidification processes which alter the microstructure prevent the initial growth structure from being examined, hence this is hard to confirm microstructurally.

To our knowledge, such an extensive transition between growth orientations with increasing undercooling has not previously been reported. However, Dantzig et al. [16] have observed an analogous transition between $\langle 100 \rangle$ and $\langle 110 \rangle$ oriented growth with increasing Zn concentration in the Al-Zn system. They refer to this as the “dendrite orientation transition (DOT)” and find that it gives rise to textured seaweed-like structures.

5. Conclusions

In summary, the results presented here reveal a number of microstructural transitions which occur with the increasing undercooling of a Cu-8.9wt%Ni alloy. Firstly, a transition from a single-grain, orthogonal dendritic microstructure to a recrystallised, equiaxed grain structure is observed at low undercooling. At intermediate undercooling this gives way to a transitional region, in which mixed $\langle 100 \rangle$ and $\langle 111 \rangle$ character dendrites are observed, with $\langle 111 \rangle$ character becoming more dominant as undercooling is increased. It seems that the competing anisotropies in the growth direction of this region are also giving rise to a novel form of the dendritic seaweed structure, characterised by its containment within a diverging split primary dendrite. At high undercooling, it is suggested that a transition to fully $\langle 111 \rangle$ growth occurs, which is accompanied by a rapid increase in growth velocity with further increases in undercooling. This, however, cannot be confirmed microstructurally due to post-solidification

modifications to the original growth structure. At the highest undercoolings achieved (up to 235 K) an equiaxed-to-elongated grain structure is observed, which may represent an intermediate structure in the spontaneous grain refinement process. Since some of the substructure appears very seaweed-like, it would appear that this might play a crucial role in this phenomenon.

References

- [1] J.L. Walker, The physical chemistry of process metallurgy, part 2, in: G.R. St. Pierre (Ed.), Interscience, New York, 1959, pp. p.845.
- [2] A.F. Norman, K. Eckler, A. Zambon, F. Gärtner, S.A. Moir, E. Ramous, D.M. Herlach, A.L. Greer, Application of microstructure-selection maps to droplet solidification: a case study of the Ni–Cu system, *Acta Materialia*, 46 (1998) 3355-3370.
- [3] K.F. Kobayashi, P.H. Shingu, The solidification process of highly undercooled bulk Cu-O melts, *Journal of Materials Science*, 23 (1988) 2157-2166.
- [4] S.E. Battersby, R.F. Cochrane, A.M. Mullis, Highly undercooled germanium: Growth velocity measurements and micro structural analysis, *Materials Science and Engineering A*, 226-228 (1997) 443-447.
- [5] N. Liu, G. Yang, F. Liu, Y. Chen, C. Yang, Y. Lu, D. Chen, Y. Zhou, Grain refinement and grain coarsening of undercooled Fe-Co alloy, *Materials Characterization*, 57 (2006) 115-120.
- [6] K.A. Jackson, J.D. Hunt, D.R. Uhlmann, T.P. Seward, Lamellar and Rod Eutectic Growth, *Trans. TMS-AIME*, 236 (1966) 149-158.
- [7] T.Z. Kattamis, M.C. Flemings, *Mod. Casting*, 52 (1967).
- [8] R.J. Schaefer, M.E. Glicksman, Direct observation of dendrite remelting in metal alloys, *Trans. AIME*, 239 (1967) 257.
- [9] M. Schwarz, A. Karma, K. Eckler, D.M. Herlach, Physical Mechanism of Grain Refinement in Solidification of Undercooled Melts, *Physical Review Letters*, 73 (1994) 1380.
- [10] A. Karma, W.-J. Rappel, Quantitative phase-field modeling of dendritic growth in two and three dimensions, *Physical Review E*, 57 (1998) 4323.
- [11] A.M. Mullis, R.F. Cochrane, On the Karma Model for Spontaneous Grain Refinement at High Solid Fractions, *International Journal of Non-Equilibrium Processing*, 11 (2000) 283-297.
- [12] A.M. Mullis, Dendritic seaweed growth and the relationship to spontaneous grain refinement, in, 2007, pp. 19-28.
- [13] Y. Sawada, Transition of growth form from dendrite to aggregate, *Physica A: Statistical Mechanics and its Applications*, 140 (1986) 134-141.
- [14] K.I. Dragnevski, R.F. Cochrane, A.M. Mullis, The solidification of undercooled melts via twinned dendritic growth, *Metallurgical and Materials Transactions A*, 35 (2004) 3211-3220.
- [15] S.E. Battersby, R.F. Cochrane, A.M. Mullis, Growth velocity-undercooling relationships and microstructural evolution in undercooled Ge and dilute Ge-Fe alloys, *Journal of Materials Science*, 34 (1999) 2049-2056.
- [16] J.A. Dantzig, P. Di Napoli, J. Friedli, M. Rappaz, Dendritic Growth Morphologies in Al-Zn Alloys. Part II: Phase-field Computations (preprint), *Metallurgical and Materials Transactions A*, Submitted (2013).

Figure Captions

Figure 1. Optical bright-field micrograph of a Cu-8.9wt%Ni sample undercooled by $\Delta T = 35$ K (top) and DIC micrograph of a sample undercooled by $\Delta T = 65$ K (bottom), with inset $\{200\}$ pole figure.

Figure 2. Optical micrographs of (top left) 8-fold nucleation pattern on the surface of a sample of Cu-8.9wt%Ni sample undercooled by $\Delta T = 139$ K and (bottom left) 6-fold nucleation pattern observed on the surface of a sample undercooled by $\Delta T = 161$ K. To the right are the corresponding $\{111\}$ pole figures.

Figure 3. An SEM montage of the branch of seaweed observed in the sample undercooled by 161 K, labelled as feature '2' in figure 3 (bottom left).

Figure 4. (Top left) DIC micrograph of a Cu-8.9wt%Ni sample undercooled by $\Delta T = 214$ K with inset $\{111\}$ pole figure, (right) optical dark field micrograph of a sample undercooled by $\Delta T = 220$ K with inset $\{111\}$ pole figure and (bottom left) enhanced DIC micrograph of dendritic seaweed observed in the region marked on the $\Delta T = 220$ K image.

Figure 5. Velocity-undercooling relationship and microstructural transitions observed in Cu-8.9wt%Ni.